Journal of Arid Environments 73 (2009) 955–962

Contents lists available at ScienceDirect

Journal of Arid Environments

journal homepage: www.elsevier.com/locate/jaridenv

Relationships between stand density and canopy structure in a dryland forest as estimated by ground-based measurements and multi-spectral spaceborne images

M. Sprintsin [a,*], A. Karnieli [a], S. Sprintsin [b], S. Cohen [c], P. Berliner [a]

[a] Jacob Blaustein Institutes for Desert Research, Ben Gurion University of the Negev, Sede Boker Campus, 84990, Israel
[b] Land Development Authority, Forest Department, Southern Region, Jewish National Found, Israel
[c] Institute of Soil, Water and Environmental Sciences, ARO Volcani Center, Bet Dagan 50250, Israel

ARTICLE INFO

Article history:
Received 2 June 2008
Received in revised form
8 April 2009
Accepted 10 April 2009
Available online 9 June 2009

Keywords:
Allometry
Clumpiness
Competition
Desert fringe
Planted forests
Remote sensing

ABSTRACT

This paper describes evaluation of forest stand density combining satellite imagery with forest inventory data set. The degree of canopy cover is described in terms of fractional vegetation cover (FVC) obtained by a linear mixture model applied on multi-spectral IKONOS image and canopy cover (CC). CC was calculated from field measurements of crown width of 646 standing trees sited within 72 circular (200 m^2) plots. A comparison between CC and FVC shows that the former can be accurately represented by the latter linking in-situ measured forest characteristics with surface reflectance measured by a satellite.

Stand density expressed as an absolute term (number of trees per unit area) showed high and significant positive correlation to FVC ($R^2 = 0.96$) and to relative density measure (Crown Competition Factor; $R^2 = 0.89$).

In order to show the applicability of the presented approach for managerial practices, a map of the spatial distribution of stand density within the forest was produced using the above-mentioned correlations. Its quality was verified against an independent data set of ground measurements. The correlation between field- and map-based number of trees per unit area was found to be satisfactory ($R^2 = 0.4$; $p < 0.05$), even though a slight lack of sensitivity was evident for low-density stands.

1. Introduction

Stand density (a measure of stem crowding within a stocked area) is one of the most important ecological characteristics of forest structure. It influences forest productivity, species establishment, stem quality and diameter (Zeide, 2005). It allows a forester to evaluate individual tree vigor (Dean and Boldwin, 1996), to predict tree form (Daniel et al., 1979), and to estimate the patterns of forest development. In addition, stand density influences the canopy clumping, which in turn affects the radiation regime within and below the overstory, influences rainfall interception, understory development, evapotranspiration, and respiration, and consequently has an important effect on stand water consumption. The latter results in long-term changes in local and global climates and feeds back to affect the vegetation growth and productivity. Early stocking reduction decreases within-stand competition and improves photosynthetic activity and water use of the remaining trees. This effect is mostly pronounced for sites pure with resources (i.e. water, nutrients, etc.) such as that in arid and semi-arid environments (Cole and Koch, 1995; Schiller et al., 2003). The sustainability of such sites is tightly related to the ability of managerial level to balance between the availability of recourses and site requirements (i.e. stocking rates, thinning and pruning regimes). In accordance with special environmental problems common in such environments (e.g. low rainfall concentrated in short periods during the year, poor and shallow soils, high temperatures and low relative humidity), landscape-level modeling is necessary to predict and optimize the benefits of dryland forestry to ecosystem stability and sustainability (Ffolliot et al., 1995). Therefore, understanding the relationships and interdependency between stand density and the structure of overstory canopy on spatial scale may be an important step towards the sustainable management of dryland ecosystems. Although, stand density can be expressed by different absolute (e.g. number of trees per unit area or basal area) and relative (e.g. Stand Density Index or 3/2 power law of self-thinning) measures (e.g. Reineke, 1933; Yoda et al., 1963), foresters around a world primarily refer to absolute measures (in particular the number of trees per unit area) as the

* Corresponding author.
E-mail address: sprintsi@bgu.ac.il (M. Sprintsin).

0140-1963/$ – see front matter © 2009 Elsevier Ltd. All rights reserved.
doi:10.1016/j.jaridenv.2009.04.011

standard parameter used for site development and monitoring. Therefore its estimation will be the main concern of this study.

Conventionally, forest structural information (on both, stand and tree levels) has been collected primarily in field surveys. This methodology is time-consuming, expensive and requires a large number of sample plots to be observed. As a result, the data obtained represent only a discrete sample in a continuous spatial domain (Salvador and Pons, 1998). In order to overcome the discontinuity problem, the possibility of estimating forest characteristics from remotely sensed data has been investigated for more than two decades (e.g. Ceccato et al., 2001; Foody et al., 2003; Ingram et al., 2005; Olsson, 1994; Sims and Gamon, 2003). The most frequently used remote sensing techniques that are relevant for forestry applications include: (1) automated photogrammetric approaches (Zagalikis et al., 2005); (2) airborne ranging radars (Cloude and Papathanassiou, 1998); and (3) airborne lasers (Hug and Wehr, 1997; Kraus and Rieger, 1999). Since the above-mentioned methods are all based primarily on airborne platforms, the data collected by them are naturally of high resolution. Though the use of such data is accurate and therefore attractive, it has at least two significant limitations. First, it is still very expensive to obtain and second, the field of view of such sensors is restricted by low altitude of platforms used. Therefore, for operational use and for covering relatively large territories it may be more convenient to utilize low cost high frequency data of lower spatial resolution, such as that obtained from spaceborne passive optical systems (e.g. Goward and Williams, 1997; Lefsky et al., 2002). However, due to estimation errors exceeding 30% (Ingram et al., 2005), these approaches have not been deemed to be satisfactory for operational use in forest management. The main reason for such errors was the low spatial resolution (usually 20–30 m per pixel) of the satellite data used (e.g. Landsat-TM/ETM+, SPOT HRV, or SPOT Pan) when compared to the size of the observation plots, which were in most cases smaller than the size of a pixel (Kayitakire et al., 2006). Therefore, recently available high spatial resolution (less than 4 m) satellite images provided by commercial satellites (e.g. IKONOS or Quickbird) have been proposed for forest management applications (Muinonen et al., 2001). However, the use of these higher resolution data for stand density estimation has still not been frequent and may be explained by the fact that most commercially available spaceborne sensors (even those with high spatial resolution) are able to observe only the surface fraction covered by the summation of tree crowns (fractional vegetation cover; FVC) rather than delineate individual crowns and count their number (Gougeon, 1995; Leckie et al., 2003). Unfortunately, vegetation fraction observed by satellites is not always linearly correlated with stand density, and statistical models to predict the latter directly from FVC require additional information, primarily about canopy sizes (Zeide, 2005). Such information is contained in relative measures of stand density, which are a direct product of the number of individuals within a specific area and their dimensions. Consequently, suggesting that these measures are more unambiguously correlated with both FVC and the number of individuals within a specific stand, we assume that their evaluation can be used as an intermediate step in assessment of number of trees per unit area from canopy fraction observations. The possibility that such two-step procedure (TSP) might be more sensitive to variations in FVC than a one-step approach (i.e. using direct correlation between vegetation fraction and stem density) allowing examination of a wider range of FVC and capturing a wider range of stem density variations will be tested in current paper.

Due to the fact that FVC can be (a) simply extracted from almost any remotely sensed data (either by linear normalization of spectral vegetation indices or by supervised or unsupervised classification of multi-spectral imagery) and (b) easily calculated from the standard inventory data set, the specific objectives of this study are to use FVC to link ground-based and remotely assessed forest characteristics in order (1) to explore the relationship between stand density and overstory development on a spatial scale and (2) to examine the potential of spaceborne multi-spectral imagery to assess forest stand density.

The proposed approach reflects the desire to anticipate end-user needs and at the same time develop an approach based on stand and canopy structure.

2. Study area

A detailed description of the study area can be found in Grunzweig et al. (2003) and Sprintsin et al. (2007). The study was carried out during March and April 2004 in a monocultured (*Pinus halepensis* Mill.) Yatir forest (31°21′ N and 35°02′ E, 630 m AMSL; ~3000 hectare area) located at the edge of the Negev and Judean deserts (Fig. 1). The mean annual precipitation rate in studied area is 275–280 mm. Rainfall is characterized by large annual fluctuations and an uneven distribution of the events within the rainy season (between November and March). Mean annual global radiation at the site is $\sim 7.5\ GJ\,m^{-2}\,y^{-1}$, mean annual relative humidity is ~40%, annual daytime maximum atmospheric vapour pressure deficit is ~1600 Pa, but ranges between <500 Pa in winter and >5000 Pa in summer (Maseyk, 2006). The average total annual potential evapotranspiration (PET) is 1600 $mm\,y^{-1}$, yielding a long-term aridity index (precipitation/PET) of ~0.17–0.18 associated with arid regions (UNEP, 1992). An average monthly temperature in the Yatir region ranges between 6.9 °C at January and 32.3 °C at July (Schiller and Cohen, 1998). The sustainability of a forest relies on the relationship between water availability and within-stand competition. The latter depends on stand structure (i.e. stand density) and totally controlled by managerial practices, primarily thinning, which reduces stand density (and to some extent the transpiring area) to the level that allows storing water in the soil also during rainless periods (Schiller and Cohen, 1995, 1998).

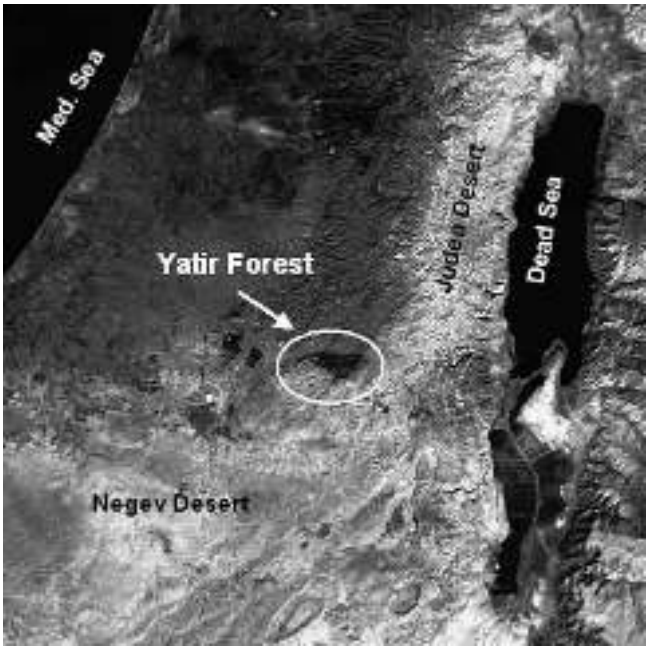

Fig. 1. Landsat-TM of Central Israel. Note the location of the Yatir forest on the desert fringe, presented as the sharp contrast between bright (arid zone) and dark tones (semi-arid zone).

3. Materials and methods

3.1. Ground-based observations

3.1.1. Sampling design, measurements and calculations

JNF's forest department provided the inventory data set. The data collection follows the traditional line-plot cruising approach with circular plot shape (Avery and Burkhart, 1983). Seventy-two circular plots of 200 m^2 each were selected within a 2 km^2 area located in the most mature ($\approx$39-year-old) central and western parts of the forest (see Fig. A.1 in Appendix 1, electronic version only) using a forest map overlaid with the network of 250 m^2 area quadrates. Training plots were located at the corner of each second quadrate. The entire set was then separated into calibration (75% of the total number of plots) and validation (25%) subsets. The exact spatial location of each plot center was determined in a field campaign using a differential Global Positioning System (dGPS) receiver with an accuracy of $\pm$2 m. The results were converted into a GIS point vector layer. Each point was then buffered by a 16-m diameter circle using MapInfo Professional (Version 7.0). As a result, a polygon layer of the training plots was produced while each plot encompasses an image footprint of approximately 4 $\times$ 4 pixels (see below).

For each tree within the selected plots DBH and crown width (CW) were measured in the following manner:

- DBH was measured 1.37 m above the ground using a caliper. Average DBH was determined by averaging two perpendicular measurements taken along the long and short axes.
- Four measurements of canopy extension (the longest observable branch) were carried out from below the canopy and averaged to obtain CW. The cross section of the canopy was assumed to be circular and CW used to compute the crown area (CA).

Canopy cover (CC) for each plot was calculated as the ratio of the sum of the crown area of all trees within a plot to the plot's area. An overlapping was clearly observed during the field campaigns indicating unevenly distributed trees and branches arrangement and emphasizing the clumpy canopy (Sprintsin et al., 2007). CC was then adjusted for canopy overlapping following Crookstone and Stage (1999) as:

$$CC = 100\left[1 - e^{(-xCC_u)}\right] \quad (1)$$

where CC is adjusted canopy cover, CC_u is unadjusted canopy cover and x is overlapping parameter taken as 0.01 (Crookstone and Stage, 1999).

For further calculation of relative density measures (see the next paragraph) the entire set of 72 plots was grouped into several DBH classes and each measured or calculated parameter was averaged per DBH class. The collected data is presented in electronic appendices Table A2.1 (Appendix 2, electronic version only).

3.1.2. Evaluation of relative stand density

The assumption of this study is that the tree crown is the only part of the tree that is visible to the remote sensor. Linking canopy cover to tree density requires, therefore, an employment of a parameter that reflects the density through a quantification of crown's interaction within particular spatial unit.

To this effect we adopted the Crown Competition Factor (CCF) that was developed by Krajicek et al. (1961) to parameterize the area available to the average tree in the stand in relation to the maximum area the tree could use if it was open-grown (Avery and Burkhart, 1983). To define the CCF the maximum crown area (MCA) concept is introduced, which is defined as the maximum crown area that a tree with a given DBH can attain. The crown competition method is based on the relation of CW (and consequently, crown area) to DBH, which can be obtained by analyzing the values measured for isolated trees, based on the assumption that there is no competition between open-growth trees (Daniel et al., 1979).

To compute CCF, the CW–DBH relationship ($CW = a \times DBH + b$, with a is a slope and b is an intercept) for 55 open-growth trees was established. Then, maximum crown area (MCA), expressed as a percent of an area an open-grown tree can occupy at a particular DBH (Avery and Burkhart, 1983), was approximated from the least-squares solution for the correlation between DBH and CW ($R^2 = 0.77$; $p < 0.01$) (Krajicek et al., 1961).

Finally, CCF was computed as the sum of MCAs divided by plot area A (m^2):

$$CCF = \frac{c\left(\sum DBH^2 N_i\right) + d\left(\sum DBH N_i\right) + e(N_i)}{A} \quad (2)$$

where N_i is the number of trees in ith DBH class, DBH (cm) is a midpoint of ith DBH class and c, d, and e are empirical constants, and the summation is carried out over the whole range of DBH classes.

A CCF of 100 indicates that the trees in the studied plot have reached their maximum possible crown development and completely utilize the ground space. A CCF below 100 indicates that the stocking rate is below its maximum potential for the specific site, assuming that the environmental conditions for the isolated growing trees and those growing in the stand are similar, while CCF exceeding 100 indicates that stands can continue their development only through a continuing loss of trees (e.g. by thinning; Avery and Burkhart, 1983). This threshold (i.e. CCF = 100), however, can be highly variable (among species) in terms of trees per unit area in an even-aged stand as the volume–cross sectional crown area relationship may vary (Daniel et al., 1979).

3.2. Satellite data acquisition and processing

A multi-spectral IKONOS image obtained on March 21, 2004 under cloud-free sky conditions was used. IKONOS has 4 spectral bands; in the blue (0.45–0.52 μm), green (0.51–0.60 μm), red (0.63–0.70 μm), and near infrared (0.76–0.85 μm) regions. An IKONOS image covers a nominal area of 16 km $\times$ 16 km at nadir with a spatial resolution of 4 m in all multi-spectral bands.

The image was radiometrically and atmospherically corrected following GeoEye company instructions (http://www.geoeye.com/products/imagery/ikonos/spectral.htm) and the 6S radiative transfer model (Vermote et al., 1997), respectively. The study area was extracted from the entire image and registered into a UTM projection by using 20 geographic control points (GSPs) obtained in the field with the dGPS receiver, resulting in average rectification errors of 0.7 and 0.85 pixels for the X and Y planes, respectively.

3.2.1. Evaluating the topographic effect on image brightness

The band rationing concept (calculating a ratio between two or more spectral bands) of spectral vegetation indices (also applied in the current research) reduces the variations in scene illumination resulting from the topographic effects. Thus, although the absolute reflectance for forest-covered slopes may vary depending on their orientation relative to the sun's position, the ratio of reflectance between the two bands should always be similar (Ouattara et al., 2004; Scheneider and Robbins, 1995). However, it also should be remembered that over some high relief and deeply shaded areas band rationing might fail to improve the effect of illumination (Colby, 1991).

The differences in image brightness for the specific case of studied image (as presented by Fig. A1.1; Appendix 1, electronic version only) prima facie could be related to topographic features. Therefore, slope, aspect (slope orientation), and shaded relief (a thematic raster image that shows variations in elevation based on a user-specified position of the sun) coverages were produced from the digital elevation model (DEM) accounting for solar zenith and solar azimuth angles (SZA and SAA respectively). These variables were produced to determine whether there is a topographic effect on the image brightness or the differences in brightness visible on IKONOS image are result of higher vegetation densities.

Each pixel of the shaded relief image is assigned a value between -1 and $+1$ indicating the amount of light reflectance at that pixel. Zero or negative values represent shadowed areas, while positive numbers represent sunlit areas. A maximum value ($+1$) was assigned to the areas of highest reflectance. Light reflectance in sunlit areas falls within a range of values depending on whether the pixel is directly facing the sun or not (ERDAS, 1999). The variation of shaded relief and Normalized Difference Vegetation Index (NDVI; Rouse et al., 1974) over the study area were investigated through analysis of the frequency distribution of NDVI values and its deviation from a normal (Gaussian) distribution by calculating skewness and kurtosis (symmetry and "peakedness" measures of the distribution relative to a normal distribution). The NDVI image and aspect coverage were then overlapped in order to examine the influence of slope orientation on vegetation development.

3.2.2. Fractional vegetation cover

A detailed description of the FVC assessment is presented in Sprintsin et al. (2007). In brief, we used a simplified two-end member Spectral Mixture Analysis (SMA) model (Roberts et al., 1998; Wu and Murray, 2003; Xiao and Moody, 2005) that consists of a single equation that presents a surface reflectance measured by a satellite as the weighted sum of canopy and background reflectance terms. These two terms are further represented by the minimum (min) and maximum (max) values of the NDVI yielding (Carlson and Arthur, 2000; Carlson and Ripley, 1997; Che and Price, 1992; Gutman and Ignatov, 1998; Price, 1987):

$$\mathrm{FVC} = \frac{\mathrm{NDVI} - \mathrm{NDVI}_{\min}}{\mathrm{NDVI}_{\max} - \mathrm{NDVI}_{\min}} \quad (3)$$

where $\mathrm{NDVI}_{\min}$ and $\mathrm{NDVI}_{\max}$ were assessed following the procedure described in detail by Gitelson et al. (2002) and Pereira et al. (2004).

3.3. Statistical analysis and evaluation of the precision of the estimations

Three quantitative methods of comparison were used to assess the precision of the estimates: (a) linear regression: the resulting 4 m resolution stand density image was overlapped with the 72 ground-measured plots' vector layer, the mean density value for each plot was extracted using a Zonal Statistics procedure from the ERDAS Imagine software and then plotted vs. corresponding ground observed value; (b) a comparison between averages of measured and modeled data sets; and (c) calculation of absolute (AE; Eq. (4)) and relative (RE; Eq. (5)) error for each pair of measured and predicted parameters.

$$\mathrm{AE} = |\mathrm{CC} - \mathrm{FVC}| \quad (4)$$

$$\mathrm{RE} = \frac{|\mathrm{measured} - \mathrm{modeled}|}{\mathrm{measured}} \quad (5)$$

4. Results

4.1. Stand density and canopy cover

The relationship between stand density and CC is presented in Fig. 2. A strong linear correlation ($R^2 = 0.96$) was found up to 53% of CC corresponding to a density of approximately seven trees per plot, the level that, possibly, points out an upper limit of the number of individuals that the site can bear or the density that was defined by forest managers as the maximum possible for current site based on resources (in particular water) availability and survival rates during the forest development.

4.2. Image data analysis

4.2.1. Topographic effect

The variation of NDVI (Table A2.1; Appendix 2, electronic version only) over the image was found to have a symmetrical (skewness $= 0.82$) and flat (kurtosis $= -0.79$) frequency distribution. This can be explained by limited range of land cover types within the area of interest, which influences the range of NDVI values ($0.13 < \mathrm{NDVI} < 0.79$). The relatively low average NDVI (0.46 ± 0.19) indicates the open nature of the studied forest, which is also characterized by low to medium FVC and stand density.

Analysis of the shaded relief image shows that shadowing does not directly affect most of the study area ($0.24 <$ shaded relief < 0.97). Moreover, the histogram of shaded relief distribution was strongly right-tailed (skewness $= 2.01$) and narrow (kurtosis $= 4.66$) with an average of 0.72 ± 0.16 with only 0.87% of the pixels having value lower (darker) than 0.6. We then suggest that the variations in image brightness are related to the distribution of vegetation canopy density over the forest, which is manifested as variation in NDVI as a function of slope degree and orientation.

4.2.2. Fractional vegetation cover

FVC was calculated according to Eq. (3) using values of 0.13 and 0.75 for $\mathrm{NDVI}_{\min}$ and $\mathrm{NDVI}_{\max}$, respectively. This resulted in a map of the spatial distribution of FVC that ranged from 0.4 to 0.7 over the study area within the entire image and averaged 0.48 ± 0.07 for the 72 training plots. This value corresponds to an average CC calculated from measured crown width of $48\% \pm 15$ (Table A2.2;

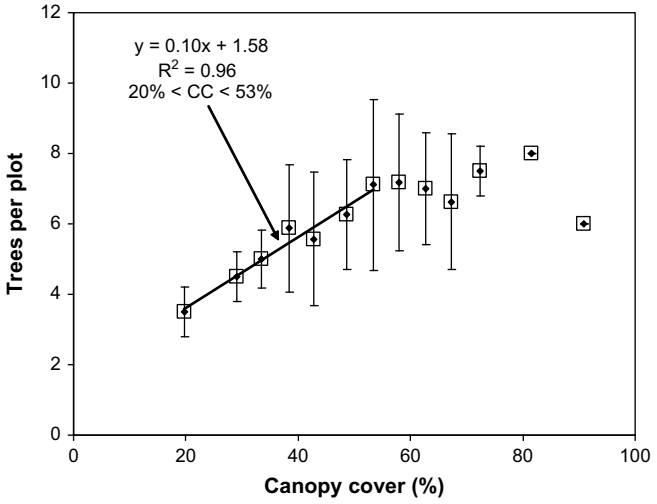

Fig. 2. The relationships between canopy cover (CC in %) and a number of trees per plot (TPP) for the cases of low to high stand density that restricts lateral growth of tree crowns.

Appendix 2, electronic version only). The average AE error was small for CC vs. FVC ($7\% \pm 4$) never exceeding 15% for per plot comparison. The correlation between CC and FVC was linear ($R^2 = 0.56$; slope $= 0.71$) and significant at $p < 0.01$ allowing the replacement of CC by FVC.

4.3. Stand density assessment and mapping

The results of the correlation between CCF and FVC (Fig. 3) clearly indicate that the linearity of the function extended beyond the one that was observed for tree density and CC, 72% compared to 53%. Within the linear range ($0.2 < \text{FVC} < 0.72$) the prediction of CCF from FVC data is feasible ($R^2 = 0.96$). An increase in FVC beyond the value of 0.72 (CCF $\sim$110), results in a slight decrease of CCF.

A per class analysis (Table A2.3; Appendix 2, electronic version only) shows that the average RE was equal to 21% (STD = 29%), while for $\sim$33% of classes it was smaller than 10% and therefore negligible. For $\sim$44% of cases, it distributed between 10 and 20%, for 11% of cases between 20 and 30%, while relative errors higher than 30% were observed for 12% of the cases. For $\sim$78% of cases the AE was less than or equal to 1 TPP and for $\sim$22% of cases it was higher. The average AE was equal to 1 TPP ($\sim$17%), which we consider sufficiently accurate for field forestry inventories. The distribution of calculated errors indicates that there is an increase towards the highest classes of DBH ($\text{AE} \geq 2$ for $\text{DBH} \geq 22$), which follows from the regressions used.

5. Discussion

5.1. Inventory data set analyses: stand density and canopy cover

The variability in CC beyond 53% for an almost constant average density of 7 TPP (Fig. 2) apparently reflects the variability in habitats that probably vary in their water holding capacities. The breakdown of linearity at CC higher than 53% limits the possibility of using this relationship for predicting TPP at high CC. This saturation level can be used as a reference when evaluating optimal stand density, because beyond it (especially over pure sites) an increase in the number of individuals may intensify mortality (e.g. Brandt et al., 2003). This might be sensitive to remote sensing methods because in such cases the background fraction observed by the satellite will increase. Consequently, a difference between red and near infrared surface reflectance measured by the sensor will be reduced (especially when understory vegetation (if any) is sparse as in the Yatir case) and the ability to relate vegetation indices to a real number of individuals per unit area will be limited.

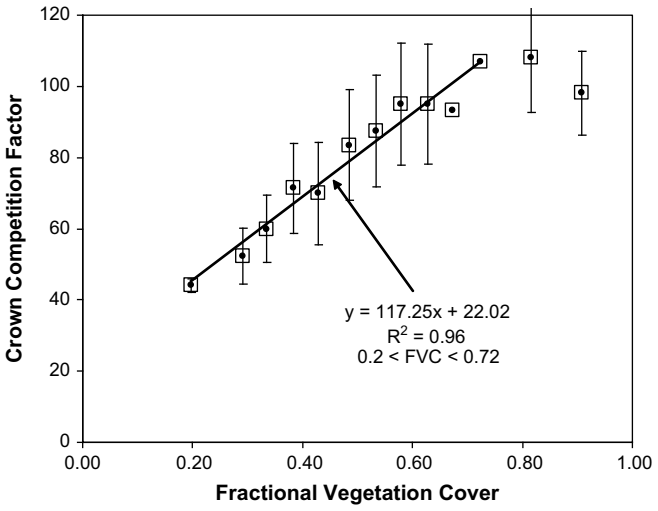

Fig. 3. Relationship between Crown Competition Factor (CCF) and fractional vegetation cover (FVC) for the Yatir forest.

Moreover, while studying the relationship between CC and stand density (by both ground- and satellite-based methods) over the forest planted in dryland, one should be aware that the functionality of such forest is non-conventional as compared to other planted forest areas (usually defined as land where trees are grown for commercial use) as it is primarily used for greening and recreation. In this case fewer trees with well developed crowns are preferable to a large number of small individuals. Thus the point of maximum TPP in Fig. 2 (TPP = 7) provides the foresters with a reference value for site status, because if the density is beyond that point, the site should be thinned for simulating crown development.

5.2. Image data analysis

5.2.1. Assessing the topography effect on image brightness

Relating the variations in image brightness to a distribution of vegetation canopy density is expectable because the solar radiance, soil types, and soil moisture are usually functions of slope steepness and aspect. Pixels in relatively low altitude or flat ground are usually located in the valley bottom and have sufficient moisture but lack direct solar radiation. A steep south-facing slope receives more solar energy but is relatively dry. Such conditions limit vegetative growth, which result in low biomass and NDVI values (Lau, 1997). In fact, no slopes steeper than 27° were found over the studied area. We then conclude that the slopes found were presumably steep enough to influence the development and survival of vegetation but at the same time sufficiently flat to have no influence on image brightness variations and consequently on further calculations of forest stand density.

Since the main regulator of forest survival in arid and semi-arid regions is water availability, it is not surprising that most of the pixels with NDVI values exceeding 0.4 were located in the North and North-West facing slopes (Fig. A1.1, inset), where low evapotranspiration rates allow soil water to be conserved for a longer period of time and thereby extended the period of relatively high biological activity and reduce mortality and the subsequent need for thinning.

5.2.2. Image-based approximation of canopy cover dynamics

We have already noted that CC can be approximated by satellite-derived FVC, which, being a substitute for CC, combines surface reflectance, with standing tree parameters and stand characteristics as defined by conventional inventory activities.

The high and significant correlation between both metrics (Fig. A1.2; Appendix 1, electronic version only) emphasizes an accuracy of remotely evaluated FVC, which was used henceforth in lieu of CC. The spread of points of the regression might be caused by the fact that when estimating CC the fraction of within-crown gaps is neglected, while FVC is an estimate of the fraction of the vegetation covered area that includes both canopy and understory (visible in gaps). The latter could lead to significant differences between both measures, particularly in sparsely vegetated areas. However, since in the area in which the study was carried out the understory vegetation cover is sparse and ephemeral (Bar Massada et al., 2006) its contribution is generally small and highly irregular over the forest.

5.3. Crown Competition Factor, stand density assessment and mapping

The breakdown in the linearity of the relationship between CCF and FVC (Fig. 3) is indicative of competition between trees and is

likely due to changes in the CW–DBH relationship, which in turn may have been affected by continuous environmental pressure (e.g. prolonged and severe drought) that damaged tree crowns. It is therefore also emphasizes the necessity of thinning, which is one of the commonly used silvicultural arrangements that lowers the rate of competition preparing a stand towards the next stress event.

A high and significant linear correlation was obtained for the relationship between tree density and CCF ($R^2 = 0.89$; $p < 0.01$). This allows us to use it in conjunction with the previously established correlation (CCF–FVC) to produce a map of stand density of the forest (for convenience TPP was converted into the number of trees per hectare (TPH; Fig. 4)). The map depicts the spatial distribution of TPH, and gives an insight into forest structure and patterns.

The analysis of the precision of stand density assessment over the validation set (summarized in Table A2.3; Appendix 2, electronic version only) shows that the average value of TPP was identical for both, counted and estimated sets (TPP = 6). However, the large difference in STD between both (1.13 for counted compared with 0.46 for estimated) emphasizes the fact that the proposed method of stem density evaluation is applicable primarily for larger scale averaging, and might not be sufficient for small areas (e.g. inventory plots). In many, if not in all, cases such large scale averaging might be more valuable for forest inventories, especially for non-timber forestry which is, having the aims of greening and landscaping, primarily focusing on development of spatial canopy extension rather than on other characteristics of individual tree (i.e. basal area, height).

5.4. Practical implementation

The approach described here requires ground truth data in order to derive the empirical equations. Those equations show that they provide accurate estimates of tree density. The potential of the approach lies in the fact that once the equations have been obtained the whole forest can be analyzed (i.e. not only the selected plots) and thus a more complete forest management policy is possible. For example, analysis of the image obtained at the first step of the research (a map of CCF, Fig. 5) could point out under- or/and over-stocked areas (marked by red circles at the figure) that remained uncovered by the network of training plots. Those areas require special attention of field crews, because their average characteristics highly exceed overall forest averages. Since for drylands the potential of overstocked sites (with CCF exceeding 100) to be affected by drought is much higher than that of sites with lower density, the remote detection and mapping of those areas provide immediate information about canopy and site status being a basis for planning pruning and/or thinning activities. Moreover, a combination of relative density characteristics with the knowledge of general site parameters (e.g. topography, soil depth and water content, etc.) gives an insight into a choosing of optimal stand density for specific site and environment.

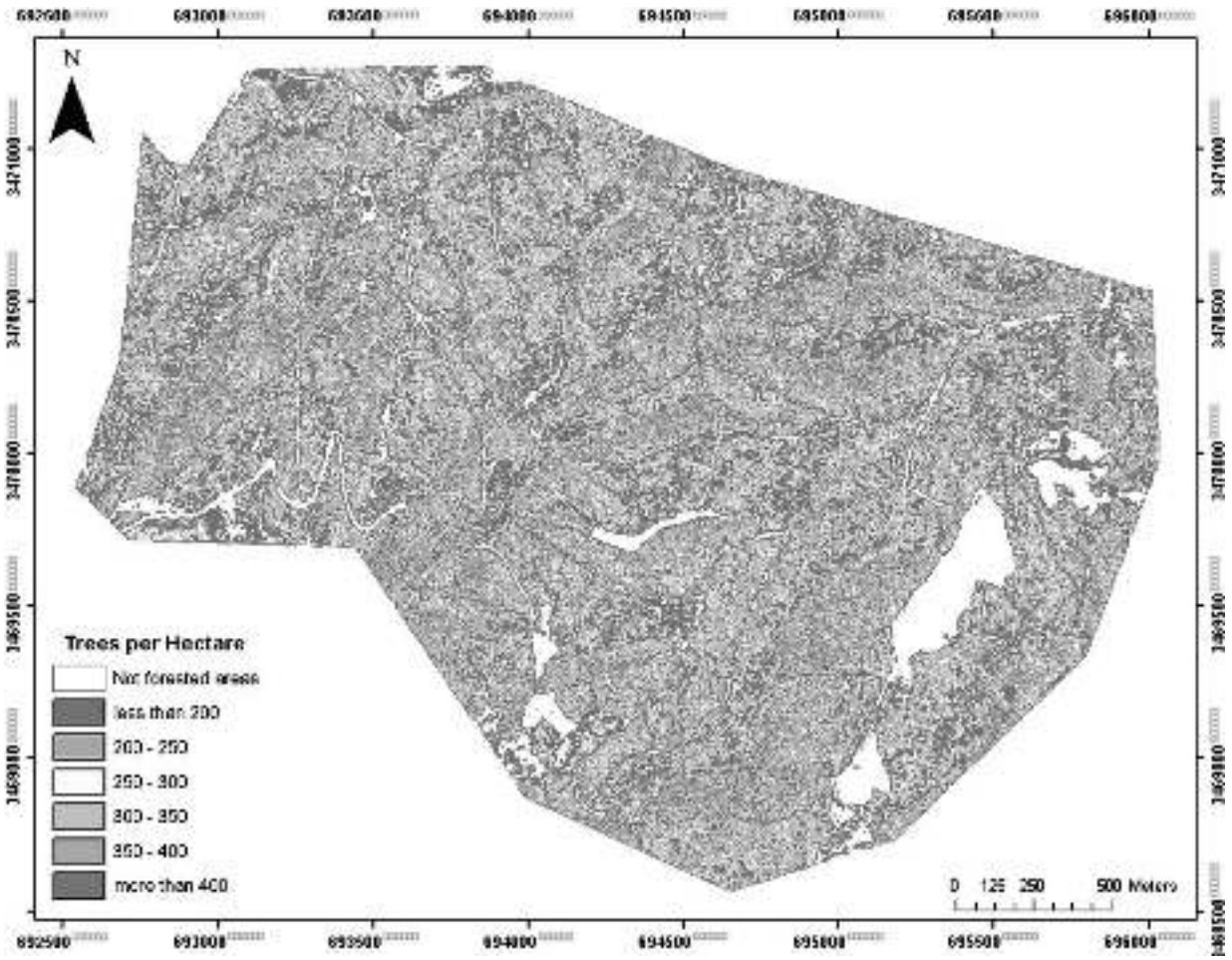

Fig. 4. Map of number of trees per hectare over the studied area in the Yatir forest.

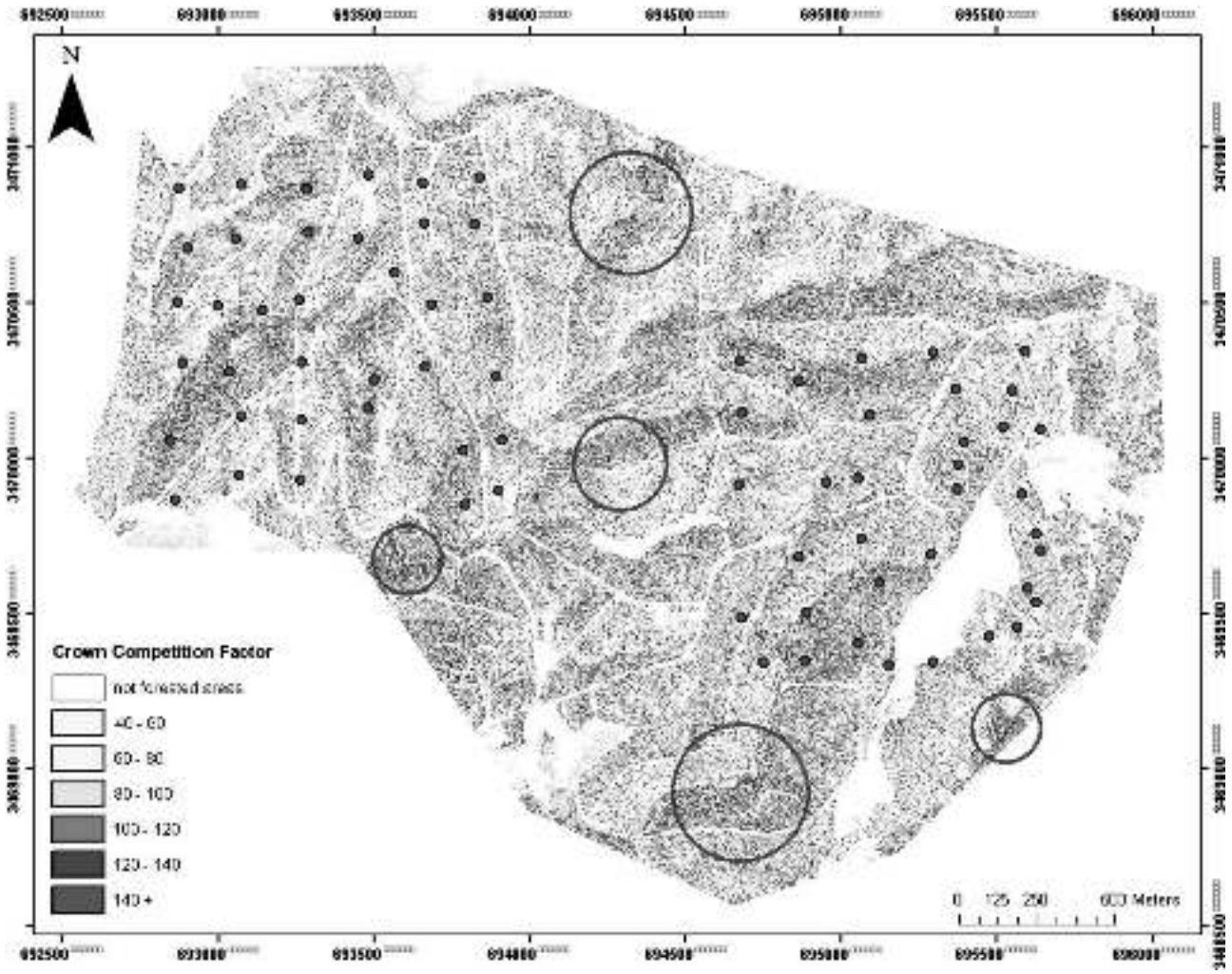

Fig. 5. Map of the Canopy Competition Factor over the studied area in the Yatir forest. Training plots presented as a red dots. Note the location of overstocked areas (red circles). (For interpretation of the references to colour in this figure legend, the reader is referred to the web version of this article.)

6. Concluding remarks

The current paper describes the application of multi-spectral remote sensing observations to describe the spatial distribution of canopy cover and presents a novel approach in estimating forest stand density. It shows that a two-step procedure (TSP) that employs the relative density measures assessment as an intermediate step to pass from satellite observations of vegetation fraction to an absolute density measure (a number of trees per unit area) is more sensitive to variations in FVC than a one-step approach (i.e. using direct correlation between vegetation fraction and stem density). It states that TSP captures a wider range of FVC and can capture a wider range of stem density variations. Such spatial evaluations may assist in determining if an area is over- or understocked regarding to resources (primarily water) availability on the one hand and management targets on the other. Moreover, since stand density is closely related to individual tree characteristics its real time estimates obtained from multi-spectral data sets can be valuable for forest surveys. Consequently, the proposed approach to forest inventory inspection fills a gap between detailed observations of small parts of forest areas and reliable techniques to extrapolate from these limited observations to the entire area of interest. It furthermore can be valuable to environmental studies especially for regional scale evaluation and monitoring of general ecosystem productivity and function.

The study confirms that a combination of conventional inventory and remote sensing methods (the techniques widely used in timber forests in northern latitudes) can be implemented with sufficient accuracy in sparse, planted, relatively homogeneous dryland forests providing a useful tool for forest management in arid and semi-arid environments. At the same time it is worth noting that an additional work is required for assessing the applicability of the proposed method for more complex terrains, mixed forests and lower spatial resolution data sets.

Appendix. Supplementary data

Supplementary data associated with this article can be found, in the online version, at doi:10.1016/j.jaridenv.2009.04.011.

References

Avery, T.E., Burkhart, H.E., 1983. Forest Measurements. McGraw-Hill, New York.
Bar Massada, A., Carmel, Y., Even Tzur, G., Grunzweig, J.M., Yakir, D., 2006. Assessment of temporal changes in aboveground forest tree biomass using areal photographs and allometric equations. Canadian Journal of Forest Research 36, 2585–2594.
Brandt, J.P., Cerezke, H.F., Mallett, K.I., Volney, W.J.A., Weber, J.D., 2003. Factors affecting trembling aspen (*Populus tremuloides* Michx.) health in the boreal forest of Alberta, Saskatchewan, and Manitoba, Canada. Forest Ecology and Management 178, 287–300.
Crookstone, N.J., Stage, A.R., 1999. Percent Canopy Cover and Stand Structure Statistics from the Forest Vegetation Simulator. USDA Publication.

Carlson, T.N., Arthur, S.T., 2000. The impact of land use–land cover changes due to urbanization on surface microclimate and hydrology: a satellite perspective. Global and Planetary Change 25, 49–65.
Carlson, T.N., Ripley, D.A., 1997. On the relation between NDVI, fractional vegetation cover, and leaf area index. Remote Sensing of Environment 62 (3), 241–252.
Ceccato, P., Flasse, S., Tarantola, S., Jacquemound, S., Gregorie, J.M., 2001. Detecting vegetation leaf water content using reflectance in optical domain. Remote Sensing of Environment 77, 22–33.
Che, N., Price, J.C., 1992. Survey of radiometric calibration results and methods for visible and near-infrared channels of NOAA-7, -9 and -11 AVHRRs. Remote Sensing of Environment 41, 19–27.
Cloude, S.R., Papathanassiou, K.P., 1998. Polarimetric SAR interferometry. IEEE Transactions on Geoscience and Remote Sensing 36 (5), 1551–1565.
Colby, J.D., 1991. Topographic normalization in rugged terrain. Photogrammetric Engineering and Remote Sensing 57, 531–537.
Cole, D.M., Koch, P., 1995. Managing Lodgepole Pine to Yielded Merchantable Thinning Products and Attain Sawtimber Rotations. USDA-Forest Service, Intermountain Research Station. Research Paper INT-RP-482.
Daniel, T.W., Helms, J.A., Baker, F.S., 1979. Principles of Silviculture, second ed. McGraw-Hill, U.S.A.
Dean, T.J., Boldwin Jr., V.C., 1996. The relationship between Reineke's stand-density index and physical stem mechanics. Forest Ecology and Management 81, 25–34.
ERDAS, 1999. ERDAS Field Guide, fifth ed. ERDAS Inc., Atlanta, GA.
Ffolliot, P.F., Gottfried, G.J., Rietveld, W.J., 1995. Dryland forestry for sustainable development. Journal of Arid Environments 30, 143–152.
Foody, G.M., Boyd, D.S., Cutler, M.E.J., 2003. Predictive relations of tropical forest from Landsat TM data and their transferability between regions. Remote Sensing of Environment 85, 463–474.
Gitelson, A.A., Kaufman, Y.J., Stark, R., Rundquist, D., 2002. Novel algorithms for remote estimation of vegetation fraction. Remote Sensing of Environment 80, 76–87.
Gougeon, F.A., 1995. A crown-following approach to the automatic delineation of individual tree crowns in high spatial resolution aerial images. Canadian Journal of Remote Sensing 21, 1–9.
Goward, S.N., Williams, D.L., 1997. Landsat and earth system science: development of terrestrial monitoring. Photogrammetric Engineering and Remote Sensing 63, 887–900.
Grunzweig, J.M., Lin, T., Schwartz, A., Yakir, D., 2003. Carbon sequestration in arid-land forest. Global Change Biology 9 (5), 791–799.
Gutman, G., Ignatov, A., 1998. The derivation of the green vegetation fraction from NOAA/AVHRR data for use in numerical weather prediction models. International Journal of Remote Sensing 19 (8), 1533–1543.
Hug, Ch, Wehr, A., 1997. Detecting and identifying topographic objects in imaging laser altimetry data. International Archives of Photogrammetry and Remote Sensing 32 (part 3–4W2), 19–26.
Ingram, J.C., Dawson, T.P., Whittaker, R.J., 2005. Mapping tropical forest structure in southeastern Madagascar using remote sensing and artificial neural networks. Remote Sensing of Environment 94, 491–507.
Kayitakire, F., Hamel, C., Defourny, P., 2006. Retrieving forest structure variables based on image texture analysis and IKONOS-2 imagery. Remote Sensing of Environment 102, 390–401.
Krajicek, L.E., Brinkman, K.A., Gingrich, S.F., 1961. Crown competition – a measure of density. Forest Science 7, 35–42.
Kraus, K., Rieger, W., 1999. Processing of laser scanning data for wooded areas. In: Fritsch, D., Spiller, R. (Eds.), Photogrammetric Week 1999. Wichmann, Heidelberg, pp. 221–231.
Lau, C.-C., 1997. Geomorphologic Distribution of Normalized Difference Vegetation Index Available at: http://www.gisdevelopment.net/aars/acrs/1997/ts10/ts10004pf.htm.
Leckie, D.G., Gougeon, F.A., Walsworth, N., Paradine, D., 2003. Stand delineation and composition estimation using semi-automated individual tree crown analysis. Remote Sensing of Environment 85, 355–369.
Lefsky, M.A., Cohen, W.B., Parker, G.G., Harding, D.J., 2002. Lidar remote sensing for ecosystem studies. BioScience 52, 19–30.
Maseyk, K.S., 2006. Ecophysiological and Phenological Aspects of *Pinus halepensis* in an Arid Mediterranean Environment. Ph.D. dissertation. Weizmann Institute of Science.
Muinonen, E., Maltamo, M., Hyppanen, H., Vainikainen, V., 2001. Forest stand characteristics estimation using a most similar neighbor approach and image spatial structure information. Remote Sensing of Environment 78, 223–228.
Olsson, H., 1994. Changes in satellite-measured reflectance caused by thinning cuttings in boreal forest. Remote Sensing of Environment 50, 221–230.
Ouattara, T., Couture, R., Bobrowsky, P.T., Moore, A., 2004. Remote Sensing and Geosciences. Geological Survey of Canada. Open file 4542.
Pereira, J.M.C., Mota, B., Privette, J.L., Caylor, K.K., Silva, J.M.N., Sá, A.C.L., Ni-Meister, W., 2004. A simulation analysis of the detectability of understory burns in miombo woodlands. Remote Sensing of Environment 93, 296–310.
Price, J.C., 1987. Calibration of satellite radiometers and the comparison of vegetation indices. Remote Sensing of Environment 21, 15–27.
Reineke, L.H., 1933. Perfecting a stand-density index for even-aged forests. Journal of Agricultural Research 46, 627–638.
Roberts, D.A., Gardner, M., Green, R.O., 1998. Mapping chaparral in the Santa Monica Mountains using multiple endmember spectral mixture models. Remote Sensing of Environment 65, 267–279.
Rouse, J.W., Haas, R.H., Schell, J.A., Deering, D.W., Harlan, J.C., 1974. Monitoring the Vernal Advancement of Retrogradation of Natural Vegetation. NASA/GCFC, Type III, Final Report, Greenbelt, MD, USA.
Salvador, R., Pons, X., 1998. On the applicability of Landsat TM images to Mediterranean forest inventories. Forest Ecology and Management 104, 193–208.
Scheneider, K., Robbins, P., 1995. GIS Mountain Environments. United Nations Institute for Training and Research, Palais des Nations, CH-1211 Geneva 10, Switzerland.
Schiller, G., Cohen, Y., 1995. Water regime of a pine forest under a Mediterranean climate. Agricultural and Forest Meteorology 74, 181–193.
Schiller, G., Cohen, Y., 1998. Water balance of *Pinus halepensis* Mill. afforestation in arid region. Forest Ecology and Management 105, 121–128.
Schiller, G., Unger, E.G., Moshe, Y., Cohen, S., Cohen, Y., 2003. Estimating water use by sclerophyllous species under east Mediterranean climate: II. The transpiration of *Quercus calliprinos* Webb. in response to silvicultural treatments. Forest Ecology and Management 179, 483–495.
Sims, D.A., Gamon, J.A., 2003. Estimation of vegetation water content and photosynthetic tissue area from spectral reflectance: a comparison of indices based on liquid water and chlorophyll absorption features. Remote Sensing of Environment 84, 526–537.
Sprintsin, M., Karnieli, A., Berliner, P., Rotenberg, E., Yakir, D., Cohen, S., 2007. The effect of spatial resolution on the accuracy of leaf area index estimation for a forest planted in the desert transition zone. Remote Sensing of Environment 109 (4), 416–428.
United Nations Environment Program, 1992. World Atlas of Desertification.
Vermote, E., Tanré, D., Deuzé, J.L., Herman, M., Morcrette, J.J., 1997. Second simulation of the satellite signal in the solar spectrum, 6S: an overview. IEEE Transactions on Geoscience and Remote Sensing 35 (3), 675–686.
Wu, C., Murray, A.T., 2003. Estimating impervious surface distribution by spectral mixture analysis. Remote Sensing of Environment 84, 493–505.
Xiao, J., Moody, A., 2005. A comparison of methods for estimating fractional green vegetation cover within a desert-to-upland transition zone in central New Mexico, USA. Remote Sensing of Environment 98, 237–250.
Yoda, K., Kira, T., Ogawa, H., Hozumi, K., 1963. Self-thinning in overcrowded pure stands under cultivated and natural conditions. Journal of Biology (Osaka City University) 14, 107–109.
Zagalikis, G., Cameron, A.D., Miller, D.R., 2005. The application of digital photogrammetry and image analysis techniques to derive tree and stand characteristics. Canadian Journal of Forest Research 35 (5), 1224–1237.
Zeide, B., 2005. How to measure stand density. Trees 19, 1–14.